21th International Conference on Renewable Energies and Power Quality (ICREPQ'23)
Madrid (Spain), 24th to 26th May 2023
Renewable Energy and Power Quality Journal (RE&PQJ)
ISSN 2172-038 X, Volume No.21, July 2023

Design of a solar mango dryer for rural sectors located in Piura-Peru

Ph.D. Freddy J. Rojas[1] B.Sc. David Huarcaya[1]

[1] Department of Mechanical Engineering
Pontifical University Catholic of Peru
Av Universitaria 1801, San Miguel 15088 (Peru)
e-mail: fjrojas@pucp.pe, a20172788@pucp.edu.pe

Abstract. In the present study, the energy design of an indirect solar dryer with the capacity to dehydrate 10 kg of mango was carried out. The methodology used was based on calculations of heat transfer, thermodynamics and dimensioning of the main components which are the solar collector and the drying chamber. As results, it was analyzed that the ambient air must enter the collector with a minimum speed of 1.175 m/s; the air increases its temperature to approximately 45 °C when passing through the collector thanks to the energy in the form of heat that is supplied, this energy being 1.363 kW, the drying process time was established in 8 hours and the environmental conditions in the Piura region were considered. Additionally, simulations were carried out that allow to know the behavior of the drying air inside the drying chamber, allowing to analyze and discuss the reason for the results that are observed graphically and numerically. It is concluded that the indirect solar dryer is a friendly option with the environment since renewable energy such as solar energy is used, thus replacing traditional dryers that generate polluting gases or use electrical sources.

Keywords. Indirect solar dryer, dehydrated mangos, numerical simulation using CFD, renewable energy-solar

1. Introduction

Currently, Peru is one of the countries that has a great diversity of fruits with approximately 623 species [1]. The production of different fruits in Peru over the last few years has allowed the agro-export sector to be placed as the second activity that generates the highest economic income in the country. However, a problem that has been observed is the loss and waste of food, also called "FLW", due to the lack of organization that exists when it comes to agricultural production, packaging, etc. Due to a bad practice at the time of production is that fruits can decompose. According to a study, it is estimated that an average of 5.6 million tons of fruits and vegetables are lost annually in Peru [2].

Regarding the production of mangoes, it is known that Peru produces mangoes mostly during the first and last quarter of the year because it takes advantage of the fact that the main generators in the market do not produce during those dates allowing to supply the international market. In addition, mango production in Peru is greater in areas of the northern coast of the country since they have a suitable climate for cultivation. The region of Piura is located in the northern part of Peru, and it was between 2000 and 2006 where an increase in the harvest area of approximately 3000 hectares was evidenced, thus making this region one of the [3].

The mango is one of the main fruits that are exported in our country and is recognized in international markets being the Kent mango the main variety of mango to be exported [3]. During the Peruvian mango campaign 2021-2022, which runs from September to April, it was possible to add the large amount of 191609 tons of mango exported worth US $ 235 million in which, compared to last season, an increase of 10% in volume and 5% in value was observed [4]. As for the export value, the average price per kilo of mango in 2020 was US$ 1.04.

A solar dryer is an equipment that allows drying by using solar radiation as an energy source to heat the air and thereby remove water from the fabrics of products such as fruits, vegetables, seeds, meat, etc. [5]. The use of a dryer of this type brings with it advantages such as being a simple and natural method since expensive equipment is not needed. There are three types of solar dryers: direct, indirect, and mixed. The direct dryer is an equipment in which a collector and a drying chamber are the same element, as a result is that the space that contains the food works as a collector receiving solar radiation [6]. The indirect dryer, unlike a direct one, has the collector and the drying chamber as individual components, the radiation affects the collector, it absorbs and stores the heat provided and with that energy it will heat the air that is led to the drying chamber where the products to be dehydrated are located. In the mixed dryer both the collector and the drying chamber directly receive solar radiation allowing it to be absorbed by the product to be dried.

There are studies in which solar dryers have been analyzed energetically. García et al. (2012) carried out the design of an indirect solar dryer that works by forced convection using a fan; they performed the selection of its components, the sizing calculations and finally dehydration tests. Other studies show the solar drying of the mango; Iglesias Díaz et al. (2017) presented the design, construction, and evaluation of a solar dryer for Ataulfo mango in which they managed to dehydrate 100 kg of mango flakes in a time of 8 hours of sunshine thus

reducing the initial humidity of the mango by approximately 72%.

In order to prevent mangoes from rotting due to decomposition and that the main producers run out of this product, it has been decided to mechanically and energetically design an indirect dehydration system that uses solar energy in the department of Piura-Peru; what you want to achieve with this drying equipment is to give it a longer life span than the mangos. The capacity of the equipment to be designed will be up to 10 kg of mango.

2. Methodology

2.1. Geographic location

The region of Piura is in the northwest of Peru, has an area of approximately 35 890 km^2, borders other departments such as Tumbes in the north, Lambayeque in the south, Cajamarca in the east and in the west with the Pacific Ocean. The latitude and longitude values of Piura are 5.1945° S and 80.6328° W respectively [7].

2.2. Weather conditions in Piura

The average values of temperature, irradiation, hours of sunshine, irradiance and relative humidity recorded in Piura from 2014 to 2021 are shown in table 1. [8][9].

Table 1. Monthly average values of parameters

Months	Temperature (°C)	Irradiation (kWh/m^2)	Hours of sunshine (h)	Irradiance (kW/m^2)	Relative humidity
Jan	26	6.3	8.7	0.724	0.62
Feb	27	6.1	8.2	0.744	0.64
Mar	27	6.1	8.8	0.693	0.64
Apr	26	6.1	9.1	0.67	0.63
May	24	6	8.7	0.69	0.63
Jun	23	5.9	7.7	0.766	0.66
Jul	21	6.2	7.4	0.838	0.66
Aug	21	6.6	7.7	0.857	0.66
Sep	21	6.9	8	0.863	0.65
Oct	22	6.9	7.9	0.873	0.64
Nov	23	6.9	8	0.863	0.64
Dec	25	6.6	8.6	0.767	0.64

2.3. Initial conditions and characteristics of solar drying equipment

The indirect solar dryer that is planned to be designed must contain two of its main components that are the solar collector responsible for collecting solar radiation and increasing the temperature of the ambient air that will be directed to the drying chamber where the mangos to be dehydrated are located.

The parameters that matter to be able to carry out the energy design and equipment sizing are the ambient temperature of the air, the temperature after passing through the solar collector, the atmospheric pressure, the relative humidity of the ambient air, the average irradiance in the environment, the drying time to be established and the initial and final humidity of the mango.

According to table 1, the average temperature will vary according to the month, so it is chosen to choose an average value of 25 °C (T_{amb}). An adequate drying temperature will depend on the size of the collector, as well as the place where it is installed. For this study, it will be taken as an initial condition that the value of the drying temperature must not exceed 60 °C since it is possible that at higher temperatures the product may enter a cooking state [10]. In addition, a drying time of 8 hours is established, as well as an average irradiance value of 0.779 kW/m^2 (I_{sol}).

It is known that the atmospheric pressure in Piura is 101.2 kPa (P_{atm}), and a relative humidity of the air of approximately 65% (HR_{amb}) is chosen.

The initial humidity of the mango is known due to the physicochemical properties of the fruit, it is worth mentioning that this value is an approximate value, since the actual initial humidity will depend on the environment from where the mango is harvested. The value of 85.5% will be taken as the initial humidity in wet base of the mango [11] ; and for the final humidity of the mango the value of 10% in wet base [12].

It is important to mention that available data of certain parameters was used in some equations, so fuzzy logic can be a useful tool to handle data affected by uncertainties and inaccuracies, since it is capable of modeling these problems through the use of fuzzy sets and disseminate the data by techniques of low computational complexity. This allows for a more realistic representation of the data and improves the accuracy and reliability of the results, especially in applications where a fast and efficient response is required [13].

2.4. Design calculations

Three important points which are part of the solar drying equipment are established. (1) is where the ambient air enters the solar collector, (2) is the outlet of the air heated by the collector entering the drying chamber, and (3) is the exit of moist air from the chamber by means of a chimney, these points are schematically in figure 1.

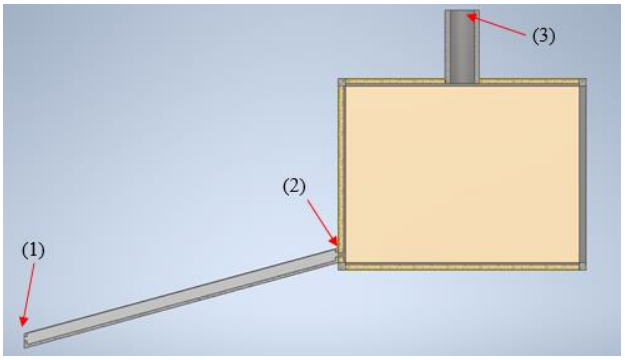

Fig.1. Diagram of inputs and outputs of the indirect solar dryer

2.4.1 Heat supplied by the collector to increase ambient air temperature

The calculations are started with the heat provided by the collector to increase the drying temperature to dehydrate the 10 kg of mango that are at the beginning. Since the temperature at the collector outlet is not known, an

expression is needed to approximate it. Equation 1 can be proposed to approximate this temperature [14].

$$\Delta T = 2\beta * (T_b - T_c) * \frac{I_{sol}}{I_o} \quad (1)$$

Where:
β =Dimensionless parameter [0.14-0.25] Optimal: 0.2
T_b = Boiling temperature of water at atmospheric pressure [100 °C]
T_c = Freezing temperature of water at atmospheric pressure [0 °C]
I_{sol} = Average solar irradiance in the area [779 W/m^2]
I_o = Solar constant [1367 W/m^2]
ΔT = Collector outlet temperature and ambient temperature difference [20 °C]

Now, it is necessary to find the amount of water that is required to evaporate using equation 2 [15].

$$m_w = \frac{m_{mango} * (M_{iw} - M_{fw})}{(1 - M_{fw})} \quad (2)$$

Where:
m_{mango} = Initial amount of mango [10 kg]
M_{iw} = Initial humidity of the mango on a wet basis [85.5%]
M_{fw} = Final humidity of the mango on a wet basis [10%]
m_w = Amount of water to be removed from the mango [8.389 kg]

Once the amount of water to be removed is found, the drying ratio (DR) can be known by dividing it by the drying time as shown in equation 3 [15].

$$DR = \frac{m_w}{t_{dry}} \quad (3)$$

Where:
t_{dry} = Drying time [8 h]
DR = Drying ratio [1.049 kg/h]

The air mass flow required for drying can also be expressed with equation 4 [15].

$$\dot{m}_{air} = \frac{DR}{\omega_3 - \omega_1} \quad (4)$$

Where:
ω_3 =Final absolute air humidity (Drying chamber outlet), kg_{water}/kg_{as}
ω_1 =Initial absolute humidity of the air (Entrance to the collector), kg_{water}/kg_{as}

As no data is known about the final relative humidity at the outlet of the drying chamber, an equation known as "Sorption Isotherms Equation" is used, which is expressed in equation 5 [12].

$$a_w = 1 - e^{\left[-e^{(0.914 + 0.5639 * \ln(M_{fd}))}\right]} \quad (5)$$

Where:
M_{fd} = Final dry air humidity [11.11 %]
a_w = Water activity [0.514]

Now, with the water activity found, the final relative humidity at the outlet of the drying chamber can be calculated with equation 6 [12].

$$HR_3 = 100 * a_w \quad (6)$$

Finally, the equation representing the total energy in the form of heat absorbed by the solar collector to heat the air is expressed in equation 7 [12].

$$E = \dot{m}_{air} * (h_2 - h_1) \quad (7)$$

Where:
h_2 = Final enthalpy of air (Collector outlet), kJ/kg
h_1 = Initial enthalpy of ambient air (Collector inlet), kJ/kg

Below is a table with the results of the above equations.

Table 2. Results for heat provided by collector

Symbol	Value	Units	Data or equation used
T_2	45	°C	(1)
T_3	34	°C	P_{atm}, HR_3, ω_3
m_w	8.389	kg	(2)
DR	1.049	kg/h	(3)
ω_1	0.01293	kg_{water}/kg_{as}	P_{atm}, HR_{amb}
ω_3	0.01733	kg_{water}/kg_{as}	h_2, HR_3
a_w	0.514	-	(5)
HR_3	51.4	%	(6)
h_1	58.02	kJ/kg	T_{amb}, HR_{amb}
h_2	78.63	kJ/kg	T_2, ω_1
$\dot{m}_{air}$	238.143	kg/hr	(4)
E	1.363	kW	(7)

2.4.2 Collector sizing

Sizing the collector refers to knowing what area this equipment needs. The area can be calculated as shown in equation 8 [16].

$$A_{col} = \frac{E}{I_{sol} * \eta_{col}} \quad (8)$$

Where:
η_{col} =Collector efficiency [50%] [17]
A_{col} = Solar collector area [3.5 m^2]

Additionally, the width (W_{col}) is defined and the length (L_{col}) of the collector is calculated, knowing that the length of the flat plate collectors is between 0.5m to 1m greater than the width, so the following will be assumed.

$$W_{col} = 1.6 \text{ m}$$

$$L_{col} = \frac{A_{col}}{W_{col}} = 2.19 \text{ m}$$

2.4.3 Angle of inclination of the collector

The necessary optimal angle of inclination (θ) can be expressed [18].

$$\theta = 10° + \text{lat}\emptyset \quad (9)$$

Where:
$lat\emptyset$ =Latitude in Piura [5.19 º]
θ = Angle of inclination with respect to the horizontal [15.19 º]

2.4. 4 Energy loss in the collector

The absorber plate is the element of the collector that contains most of the solar energy, so an energy balance is proposed to know how much the loss is it has. Using equation 10, this loss can be calculated [18].

$$I_{sol} * A_{col} * (\tau * \alpha) = Q_u + Q_L + Q_s \quad (10)$$

Where:
τ =Transparent cover transmissivity [0.85] [19]
α =Absorbing plate absorptivity [0.9] [18]
Q_u = Useful energy for heating air (Q_u = E) [1.363 kW]
Q_s = Stored energy [0 kW]
Q_L = Energy lost by conduction, convection, and re-radiation waves [0.723 kW]

2.4.5 Minimum required drying air velocity

It will be calculated how much is the speed that the air needs to be able to work under the given conditions. First, the volumetric flow is calculated with equation 11.

$$\dot{V}_{air} = \frac{\dot{m}_{air}}{\rho_{air}} \quad (11)$$

Where:
ρ_{air} = Air density at collector inlet [1.173 kg/m^3]
$\dot{V}_{air}$ = Volumetric air flow [0.056 m^3/s]

The minimum velocity required (v_{inl_air}) for the above calculated flow to exist is calculated by dividing this flow by the air inlet area (A_{inl_air}) of the collector. The corresponding equations for the calculation are equations 12 and 13.

$$A_{inl\_air} = B_{air} * H_{air} \quad (12)$$

$$v_{inl\_air} = \frac{\dot{V}_{air}}{A_{inl\_air}} \quad (13)$$

Where:
W_{air} = Air inlet width [1.6 m]
H_{air} = Air inlet height [0.03 m]
A_{inl_air} = Air inlet area [0.048 m^2]
v_{inl_air} = Minimum air inlet velocity [1.175 m/s]

2.4.6 Drying chamber sizing

This calculation is related to the amount of mango to be placed, the number of trays, as well as their dimensions and other influencing factors. First, the drying area inside the chamber will be sized, which is the total area in which the mango must be located to be dehydrated. The drying area is calculated with equation 14 [19].

$$A_{dry} = \frac{m_{mango}}{\rho_{mango} * e_{mango} * \zeta * (1 - \varepsilon_v)} \quad (14)$$

Where:
ρ_{mango} = Mango density [1057.8 kg/m^3]
e_{mango} = Thickness of the product layer on the tray [0.015 m]
ζ =Porosity of the mango [0.066] [20]
ε_v = Empty space factor [0.3]
A_{dry} = Total drying area [13.652 m^2]

With the calculated drying area, 6 trays were chosen to accommodate them in the drying chamber. Also, dividing the drying area by the number of trays will find the area needed on each tray.
$\#trays = 6$

$$A_{tray} = \frac{A_{dry}}{\#trays} \quad (15)$$

Assuming that the width of each tray (W_{tray}) is 1.5 m, the length of the trays (L_{tray}) can be calculated by substituting into equation 15.

$$1.5 * L_{tray} = \frac{13.652}{6}$$

$$L_{tray} = 1.517 \text{ m} \approx 1.52 \text{ m}$$

Knowing the dimensions that the trays will have and knowing that the width of the drying chamber must be equal to the width of the calculated collector is that the following dimensions are taken.

$$L_{chamber} = 1.6 \text{ m}$$

$$W_{chamber} = W_{col} = 1.6 \text{ m}$$

$$H_{chamber} = 1.2 \text{ m}$$

2.4.7 Pressure drop in the drying chamber

The difference in air pressure from the inlet of the drying chamber to its exit through the chimney can be expressed with equation 16 [21].

$$\Delta P_{chamber} = 0.0038 * g * (T_2 - T_{amb}) * H_{chamber} \quad (16)$$

Where:
g = Gravity [9.81 m/s^2]
$\Delta P_{chamber}$ = Air pressure drop in the drying chamber. [1.267 Pa]

2.4.8 Energy loss in the drying chamber

The internal and external convective coefficients must be calculated to perform the heat transfer equation and find the amount of heat going outside.

Calculation of internal convective coefficient

Since the airflow passes through a square section, the hydraulic diameter (D_{hid}) will be equal to the side of the square section equivalent to 1.6 m. On the other hand, the reference temperature for this calculation is the average of the chamber inlet and outlet temperatures (T_{ave}) as shown in equation 17.

$$T_{ave} = \frac{T_2 + T_3}{2} \quad (17)$$

$T_{ave} = 39.5$ °C

Then, the Reynolds number inside the drying chamber is calculated with equation 18.

$$Re_{int} = \frac{\rho_{int} * v_{ent\_air} * D_{hid}}{\mu_{int}} \quad (18)$$

Where:
ρ_{int} = Air density inside the drying chamber [1.118 kg/m^3]
μ_{int} =Dynamic viscosity of the air inside the drying chamber [1.913*10^{-5} kg/m*s]
Re_{int} =Number of Reynolds inside [1.099*10^5]

Since it is true that $10000 \leq Re_{int} \leq 5 * 10^6$ and $0.5 \leq Pr_{int} \leq 1.5$, the Gnielinski equation expressed in equation 19 for gases is applied to find the Nusselt number.

$$Nu_{int} = 0.0214 * \left(Re_{int}^{0,8} - 100\right) * Pr_{int}^{0,4} \quad (19)$$

Where:
Pr_{int} = Prandtl number inside [0.7416]
Nu_{int} =Nusselt number inside [202. 819]

Finally, the internal convective coefficient is calculated with equation 20.

$$\alpha_{int} = \frac{Nu_{int} * k_{int}}{D_{hid}} \quad (20)$$

Where:
k_{int} =Coefficient of conductivity of the air inside the chamber [0.02666 W/m*K]
α_{int} =Internal convective coefficient of air [3.79 W/m^2*K]

Calculation of external convective coefficient

For this calculation, the ambient air temperature is taken as a reference. In addition, the wind speed (air) outside is determined by weather conditions.

$$v_{air\_amb} = 9\ \frac{km}{h} = 2.5\ \frac{m}{s}$$

The Reynolds number outside the drying chamber is calculated with equation 21.

$$Re_{ext} = \frac{\rho_{ext} * v_{air\_amb} * D_{hid}}{\mu_{ext}} \quad (21)$$

Where:
ρ_{ext} = Air density outside the drying chamber [1.173 kg/m^3]
μ_{ext} = Dynamic viscosity of the air outside the drying chamber [1.846*10^{-5} kg/m*s]
Re_{ext} = Number of Reynolds exterior [2.542*10^5]

Equation 22 is used to calculate the Nusselt number since $Re_{ext} \leq 5 * 10^5$

$$Nu_{ext} = 0.332 * Re_{ext}^{\frac{1}{2}} * Pr_{ext}^{\frac{1}{3}} \quad (22)$$

Where:
Pr_{ext} = Number of Prandtl exterior [0.7427]
Nu_{ext} =Number of Nusselt exterior [151.579]

Finally, the external convective coefficient is calculated with equation 23.

$$\alpha_{ext} = \frac{Nu_{ext} * k_{ext}}{D_{hid}} \quad (23)$$

Where:
k_{ext} =Air conductivity coefficient outside the chamber [0.02557 W/m*K]
α_{ext} =External convective coefficient of air [2.422 W/m^2*K]

Once the convective coefficients have been calculated, the overall transfer coefficient from the inside to the outside is calculated. For the analysis of this coefficient, a diagram with the surfaces in the drying chamber that are in contact with air is shown in the following figure 2.

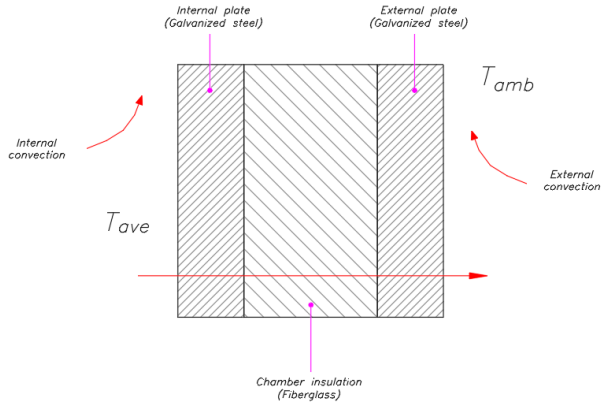

Fig.2. Scheme of the walls of the drying chamber

The thickness and conductivity of the materials of the internal insulation (fiberglass) and of the plates of the internal and external chamber (galvanized steel) that make up the walls of the drying chamber are defined. Then, the global transfer coefficient is calculated with equation 24.

$$U = \frac{1}{\left(\frac{1}{\alpha_{int}}\right) + \left(\frac{e_{plate\_int}}{k_{st\_galv}}\right) + \left(\frac{e_{insulation}}{k_{fib\_glass}}\right) + \left(\frac{e_{plate\_ext}}{k_{st\_galv}}\right) + \left(\frac{1}{\alpha_{ext}}\right)} \quad (24)$$

Where:
$e_{insulation}$ = Chamber insulation thickness [30 mm]
e_{plate_int} = Thickness of the internal plate of the chamber [5 mm]
e_{plate_ext} = Thickness of the external plate of the chamber [5 mm]
k_{fib_glass} = Thermal conductivity of fiberglass [0.041 W/m*K]
k_{st_galv} = Thermal conductivity of galvanized steel [47 W/m*K]
U = Overall transfer coefficient [0.694 W/m^2*K]

The total area of the chamber walls (A_{walls}) that are in contact with the airflow is expressed in equation 25.

$$A_{walls} = 2 * (L_{chamber} * W_{chamber} + W_{chamber} * H_{chamber} + L_{chamber} * H_{chamber}) \quad (25)$$

$A_{walls} = 12.8\ m^2$

Finally, the heat lost by convection and conduction in the drying chamber ($Q_{lost\_chamber}$) is calculated with equation 26.

$$Q_{lost\_chamber} = U * A_{walls} * (T_{ave} - T_{amb}) \quad (26)$$

$Q_{lost\_chamber} = 128.823\ W$

2.4.9 Heat to dehydrate mango

The heat needed to dehydrate the mango refers to the heat that the air that was heated in the solar collector will provide to the mango by heat transfer for water evaporation. The amount of heat can be divided into heat to preheat the mango and the heat needed to evaporate the water. The formula for finding heat to preheat the mango [22].

$$Q_{pre\_heat} = \frac{m_{mango} * cp_{mango} * (T_{f\_mango} - T_{i\_mango})}{t_{dry}} \quad (27)$$

Where:
T_{f_mango} = Final mango temperature [318 K]
T_{i_mango} = Initial mango temperature [298 K]
cp_{mango} =Specific heat of the mango [3.77 kJ/kg*K]
Q_{pre_heat} = Heat to preheating the mango [0.026 kW]

On the other hand, the necessary heat needed to evaporate the water from the mango is shown in equation 28.

$$Q_{evap} = \frac{m_w * h_{fg}}{t_{dry}} \quad (28)$$

Where:
h_{fg} = Latent heat of water vaporization [2404 kJ/kg]
Q_{evap} = Heat to evaporate water from the mango [0.7 kW]

Adding both terms, the total heat necessary to dehydrate the mango is obtained (Q_{deh_mango}) and the formula can be seen in equation 29.

$$Q_{deh\_mango} = Q_{pre\_heat} + Q_{evap} \quad (29)$$

$Q_{deh\_mango} = 0.726\ kW$

Figure 3 shows a modeling of the indirect solar dryer formed by the solar collector and the drying chamber.

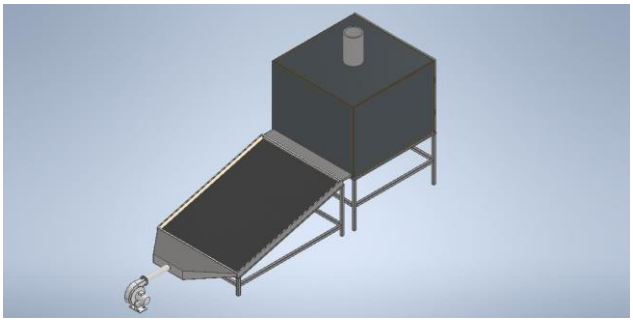

Fig.3. Indirect solar dryer

3. Simulation

The simulation allows to observe how the air, after being heated in the solar collector, passes through the drying chamber where the mango slices will be located. Using the Ansys Workbench 2022 software, the results of the simulation of parameters such as temperature, speed and pressure will be obtained; the results obtained will be analyzed in order to know the behavior of the air circulating inside the system.

Analyzing the temperature values first, the temperature contour can be seen in figure 4 in a symmetrical plane that divides the dryer into two halves.

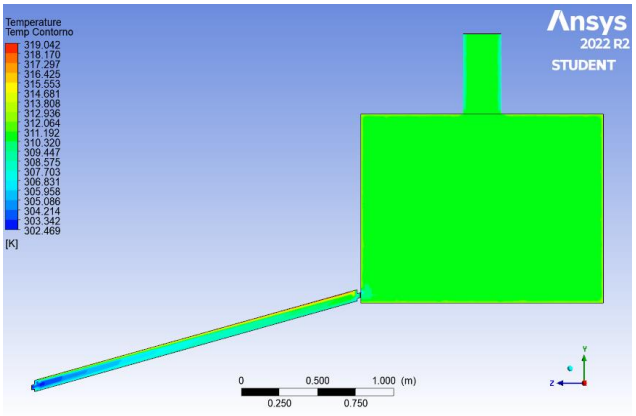

Fig.4. Temperature contour in the dryer

There is an increase in temperature as planned, and that the temperature value in the chamber is approximately uniform. It is observed that the temperature value at the exit of the collector goes between 311 K and 313 K (38 ºC and 40 ºC), these values are lower than the calculated one which was 45 ºC, the reason is because in the simulation the value of a specific day is taken to be able to take the irradiation of that day, unlike the numerical calculation where the average value of the months of the year was taken. The value at the exit of the solar dryer that is expelled through the chimney according to the simulation is 37.556 ºC (310.556 K), this value is higher by 3.556 ºC to the previously calculated which was 34 ºC, the reason for this is because in this simulation the interaction with the mango or with the trays where the air will flow is not taken into account, this causes the air, when encountering bodies that produce a type of resistance and dissipation to heat, to decrease its temperature, thus being able to explain the reason for this value a little higher.

Additionally, it can be considered how the temperature distribution occurs in horizontal planes located in the drying chamber, this in order to observe that this parameter is uniform in the planes, since this allows to intuit that the dehydrated will also be uniform which is something beneficial since it will be achieved that the mango slices obtain a very similar final moisture content and without many deviations. The plans that were worked on were on the ZX axis, 3 planes were worked in total, strategically located in the lower, middle and upper part of the drying chamber to know the temperature distribution in these parts. The following figures show how the air temperature is distributed in the mentioned planes.

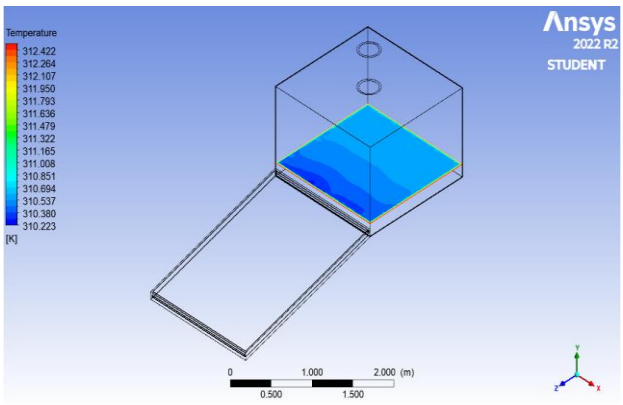

Fig.5. Temperature distribution in a low plane of the drying chamber

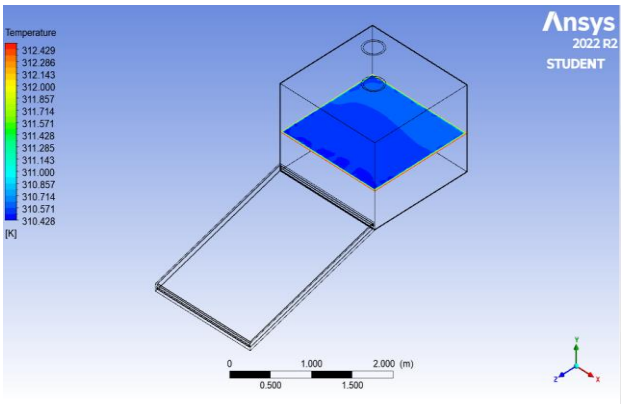

Fig.6. Temperature distribution in a midplane of the drying chamber

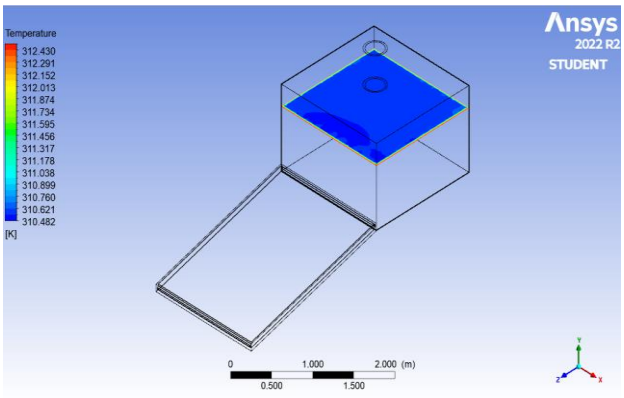

Fig.7. Temperature distribution in a high plane of the drying chamber

From figures 5,6 and 7 it can be known that the distribution of temperatures in the planes is uniform, there is a more noticeable variation of temperature in the low plane because this plane is the one that is closest to the air outlet of the collector causing the air to concentrate in the back of the plane and thus existing this slight difference. As the medium and high planes are analyzed, it can be seen that the uniformity is increasing, the reason for this phenomenon is that the air temperature is closer and closer to the outlet chimney, being much closer to the ambient air, which causes not only greater uniformity, but also a small decrease in temperature compared to that obtained in the low plane.

Knowing the mass flow of air required at the collector inlet ($\dot{m}_{air}$) it is possible to know the value of the inlet velocity.

In addition, the distribution of the speed in the drying chamber can be known thanks to the simulation carried out and with the help of flow lines, this simulation gives an idea of the direction and numerical value of the speed. Figure 8 shows the air flow lines that circulate through the drying chamber.

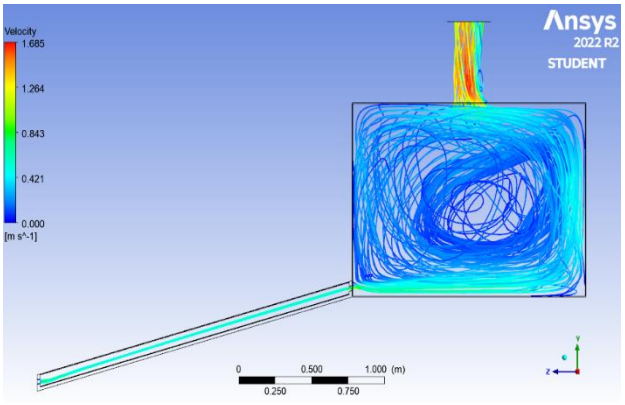

Fig.8. Air flow lines in the drying chamber

From figure 8 it can be seen how the distribution and speed values are given in the drying chamber. There is a tendency of the air that leaves the collector, this tendency is to flow through the lower wall of the drying chamber until it reaches the rear wall of the same, once it reaches the rear the air flow goes in a vertical direction towards other walls such as the sides and the top, This phenomenon is known as recirculation and is linked to drying processes. Brazil Maia et al. (2012) show a very similar behavior of the air flowing in the drying chamber, they also show that it is because of this recirculation that the temperature tends to be higher at the back of the chamber.

The pressure of the air that enters the chamber is a parameter that indicates with what force the fluid impacts against the various bodies that will be found such as trays and mangos slices. Because there is a proportional relationship between pressure and temperature, it can be identified that the pressure must also be approximately uniform, this can be seen in figure 9 in which the pressure contour can be seen in a plane that divides the dryer .

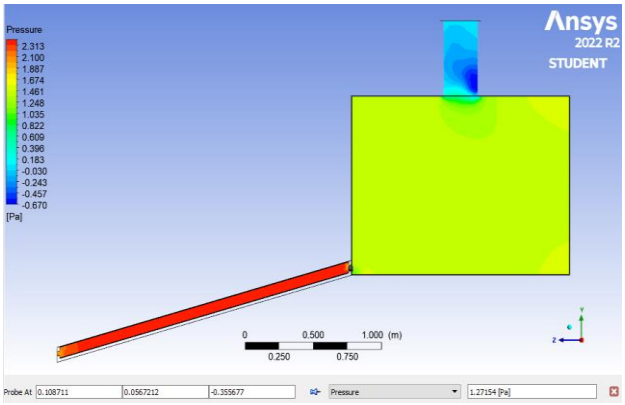

Fig.9. Pressure contour in the dryer

From the previous figure it can be seen that there is an almost uniform pressure in the chamber. Additionally, in the previous calculations it was found what would be the drop in pressure of the air that crossed the chamber

($\Delta P_{chamber}$), this value can be compared with that obtained in the simulation. Due to the use of the boundary condition at the exit with 0 Pa, it can be affirmed that the inlet pressure to the chamber is equal to the pressure difference that exists in it. In figure 9, additionally, the pressure value of the point located at the entrance of the chamber is 1.2715 Pa; the difference between the pressure values of the simulation and the calculated one is 0.0045 Pa, being a minimum difference.

4. Discussion

In the study by García et al. (2012) when calculating the sizing of the solar collector, the value of 80% efficiency of the flat solar collector is taken, this value is high since the average efficiency values are between 40 and 60%, this due to the heat losses that exist in the process of heating the air. On the other hand, in this study a centrifugal fan was chosen that will allow to generate the forced convection of the air that will enter the collector, this in order to have a better efficiency since the air circulation is increased, the drying time is reduced and an increase in the temperature of the drying air is generated.

According to Iglesias Díaz et al. (2017) the result of the air flow used in its analysis is inversely proportional to the drying temperature obtained after heating the ambient air since for a uniform drying there must be a relationship between the air speed and the drying temperature, this is evidenced in this study also since for an air flow of 238.143 kg/hr (0.0661 kg/s) the air was heated to an average temperature of 45 ºC, while in the study by Iglesias Díaz et al. (2017) has an air flow of 0.042 kg/s at a drying temperature of 323 K (50 ºC), there is a relationship between the values shown.

5. Conclusions

The indirect solar dryer designed allows to dehydrate 10 kg of mango slices per day with a drying time of approximately 8 hours in which there is an average irradiance value of 779 W/m^2. Being an indirect dryer it is possible to obtain a better quality product since the radiation is used as a source to heat the air that will come into contact with the mango slices, unlike a direct dryer in which the radiation directly impacts the fruit, being almost non-existent the control of the process.

The use of a flat plate solar collector turned out to be the most suitable equipment for dehydration since the heating temperature of the air is within the working range of this collector; in addition, it allowed the capture of solar radiation with an area of 3.5 m^2 and an absorbed heat of 1.363 kW to heat the air. On the other hand, the drying chamber contains 6 trays of area 2.275 m^2 each stacked vertically and separated 15 cm from each other allowing to place the fruit that will go from an initial humidity of 85.5% to a final humidity of 10%. It is important to know and understand the requirements of the project such as the amount to be dehydrated, the place of operation, among others to achieve an optimal design that is adequate in order to take advantage of radiation as an energy source.

The simulation allowed to analyze the thermal behavior of the air and corroborate the analytical calculations developed, obtaining that the simulated temperature at the exit of the collector is between 38 ºC and 40 ºC, a value similar to the analytical calculation that was approximately 45 ºC. In addition, there are other values that were corroborated such as the speed of entry into the dryer or the pressure drop in the drying chamber, so it is concluded that the calculations of the air in the inlets and outlets of the dryer were developed appropriately.

6. Acknowledgment

We thank the Pontificia Universidad Católica del Perú for their support in preparing the project.

References

[1] Ministerio de Desarrollo Agrario y Riego, “Frutas,” 2015. https://www.midagri.gob.pe/portal/32-sector-agrario/frutas (accessed Apr. 01, 2022).

[2] N. S. Bedoya-Perales and G. P. Dal’ Magro, “Quantification of Food Losses and Waste in Peru: A Mass Flow Analysis along the Food Supply Chain,” *Sustain. 2021, Vol. 13, Page 2807*, vol. 13, no. 5, p. 2807, Mar. 2021, doi: 10.3390/SU13052807.

[3] Ministerio de Desarrollo Agrario y Riego, “Mangos,” 2015. https://www.midagri.gob.pe/portal/186-exportaciones/evolucion-de-las-exportaciones-de-los-principales/606-mangos (accessed Apr. 13, 2022).

[4] Fresh Fruit, “Campaña del mango mejora, pero sigue por debajo de niveles prepandemia,” 2022. https://freshfruit.pe/2022/02/06/campana-del-mango-mejora-pero-sigue-por-debajo-de-niveles-prepandemia/#:~:text=La campaña peruana de mango,toneladas por US%24 235 millones.

[5] U. Unidad de Ecotecnologías, “Deshidratadores Solares .” https://ecotec.unam.mx/ecoteca/deshidratadores-solares-2 (accessed Apr. 16, 2022).

[6] Cocina Solar, “Deshidratador solar y Secado solar de alimentos,” 2018. https://gastronomiasolar.com/deshidratador-solar-secado-alimentos/ (accessed Apr. 13, 2022).

[7] Geodatos, “Coordenadas geográficas de Piura ,” 2022. https://www.geodatos.net/coordenadas/peru/piura (accessed Nov. 10, 2022).

[8] Weather Spark, “El clima y el tiempo promedio en todo el año en Piura,” 2022. https://es.weatherspark.com/y/18257/Clima-promedio-en-Piura-Perú-durante-todo-el-año (accessed Aug. 24, 2022).

[9] Climate-Data, “Clima Piura,” 2021. https://es.climate-data.org/america-del-sur/peru/piura/piura-3403/ (accessed Aug. 24, 2022).

[10] A. De Michelis and E. Ohaco, “Definiciones y algunos conceptos básicos,” *Deshidratación y desecado frutas, hortalizas y hongos. Procedimientos hogareños y Comer. pequeña escala*, 2012, [Online]. Available: https://inta.gob.ar/sites/default/files/script-tmp-inta_cartilla_secado.pdf

[11] L. A. Bautista and D. F. Meza, “Diseño y construcción de una deshidratadora automática para frutas y verduras para la empresa SENSORTECSA S.A.,”

Universidad de las Fuerzas Armadas ESPE, 2016. Accessed: Mar. 31, 2022. [Online]. Available: http://repositorio.espe.edu.ec/handle/21000/11606

[12] E. O. M. Akoy, M. Ismail, E.-F. Ahmed, and W. Luecke, “Design and Construction of A Solar Dryer for Mango Slices,” vol. 4, no. November, pp. 1946–1951, 2015.

[13] F. C. Morabito, M. Versaci, G. Pautasso, and C. Tichmann, “Fuzzy – neural approaches to the prediction of disruptions in ASDEX Upgrade,” vol. 1715, 2001.

[14] I. C. Macedo and C. A. C. Altemani, “Experimental evaluation of natural convection solar air heaters,” *Sol. Energy*, vol. 20, no. 5, pp. 367–369, 1978, doi: 10.1016/0038-092X(78)90151-2.

[15] M. Al-Busoul, “Design of Fruits Solar Energy Dryer under Climatic Condition in Jordan,” *J. Power Energy Eng.*, vol. 05, no. 02, pp. 123–137, 2017, doi: 10.4236/jpee.2017.52007.

[16] L. E. García, M. F. Mejía, D. J. Mejía, and C. A. Valencia, “Diseño y construcción de un deshidratador solar de frutos tropicales,” *Av. Investig. en Ing.*, vol. 9, no. 2, pp. 9–19, 2012.

[17] M. A. Leon, S. Kumar, and S. C. Bhattacharya, “A comprehensive procedure for performance evaluation of solar food dryers,” *Renew. Sustain. Energy Rev.*, vol. 6, no. 4, pp. 367–393, 2002, doi: 10.1016/S1364-0321(02)00005-9.

[18] O. J. Alamu, C. N. Nwaokocha, and O. Adunola, “Design and Construction of a Domestic Passive Solar Food Dryer,” *Leonardo J. Sci.*, no. 16, pp. 71–82, 2010, [Online]. Available: http://ljs.academicdirect.org/A16/071_082.htm

[19] F. M. Claros, “Colector Solar de Placa Plana,” pp. 67–77, 1981.

[20] M. C. Rodríguez, L. F. Guardiola, and R. Pacheco, “Aplicación De La Ingeniería De Matrices En La Fortificación De Mango (Var. Tommy Atkins) Con Calcio,” *Dyna*, vol. 74, no. 153, pp. 19–26, 2008, [Online]. Available: http://www.revistas.unal.edu.co/index.php/dyna/article/view/936/11628

[21] V. K. Jindal and S. Gunasekaran, “Estimating Air Flow and Drying Rate Due to Natural Convection in Solar Rice Dryers.” 1982.

[22] W. Wang, M. Li, R. H. E. Hassanien, Y. Wang, and L. Yang, “Thermal performance of indirect forced convection solar dryer and kinetics analysis of mango,” *Appl. Therm. Eng.*, vol. 134, pp. 310–321, 2018, doi: 10.1016/j.applthermaleng.2018.01.115.

[23] C. Brasil Maia, A. Guimarães Ferreira, L. Cabezas-Gómez, S. de Morais Hanriot, and T. de Oliveira Martins, “Simulation of the Airflow Inside a Hybrid Dryer,” *Int. J. Res. Rev. Appl. Sci.*, vol. 10, no. March, pp. 382–389, 2012, [Online]. Available: http://arpapress.com/Volumes/Vol10Issue3/IJRRAS_10_3_02.pdf

[24] R. Iglesias Díaz, R. A. José Gómez, O. Lastres Danguillecourt, P. López de Paz, N. Farrera Vázquez, and G. R. Ibáñez Duharte, “Diseño, construcción y evaluación de un secador solar para mango Ataulfo,” *Rev. Mex. Ciencias Agrícolas*, vol. 8, no. 8, pp. 1719–1732, 2017, doi: 10.29312/remexca.v8i8.697.